Sample preparation

$FeSO_4 \cdot 7H_2O$, KNCS and ligand abpt were purchased and used without further purification. MeOH used for synthesis was added in small amount of ascorbic acid to prevent the oxidation of Fe^{2+}. The compounds were synthesized by slow diffusion between two layers of solution in a test tube. The bottom layer contained Fe^{2+} (0.01 mmole) / NCS^- (0.02 mmole) in 10 ml of 1:1 H_2O / MeOH, which was prepared by filtering off K_2SO_4 after mixing $FeSO_4 \cdot 7H_2O$ and KNCS in MeOH and stirred for 15 min. The top layer contained stoichiometric amounts of abpt (0.02 mmole) in 10 ml of MeOH. After a week, crystals of title compounds were obtained by filtering, which contain the major product of polymorph **D**, but occasionally small amount of **A** or **B** yield simultaneously. Single crystals of polymorph **A** , **B** and **D** can be easily distinguished by the color and morphology of the crystal. **A** is dark-red in block shape; **B** is orange in rhombohedron; and the color of **D** is in-between with needle shape. Samples used for physical property measurements and crystals suitable for X-ray diffraction are separated manually under the microscope. As for polymorph **C**, which can only be crystalized with very slow diffusion rate in low concentration of starting materials.

Crystallographic experiment

Single crystal diffraction data were collected on an in-house Bruker-Kappa CCD diffractometer using graphite-monochromated Mo$K\alpha$ radiation. A Helix cryosystem (Oxford Cryosystem) was used for data measurements of polymorph **C** at 25, 60 and 130K. An Oxford liquid nitrogen cryosystem was used for data collection of **D** at 100K. The nozzle of the Helix cryosystem is very close to the sample crystal, which does prohibit part of the goniometer setting angles and results in low completeness. Software DENZO were used to integrate the diffraction intensity, the absorption correction was applied using SORTAV for polymorph **C** and SADABS for **D**. The structures were solved by direct methods and refined with full-matrix least squares based on F^2 using SHELXS and SHELXL respectively. All non hydrogen atoms were refined anisotropically. Hydrogen atoms on the pyridyl rings were treated by riding model and not refined, while the H atoms of amino group were located in difference Fourier maps and refined isotropically.

Crystal data:

Crystal data for polymorph **C** at T = 300(2) K: $C_{26}H_{20}N_{14}S_2Fe$, M = 648.53, monoclinic, space group $P2_1/c$, a = 16.4000(3), b = 17.5754(3), c = 9.9940(2) Å, β =

90.748(1)º, V = 2880.33(9) Å^3, Z = 4, F(000) = 1328, D_{cacld} = 1.496 g cm^{-3}, μ(Mo–K$_\alpha$) = 0.714 mm^{-1}, 2θ_{max} = 54.96°. Red-brown in block (0.45 × 0.30 × 0.20 mm^3). 26033 total reflections, 6573 independent reflections (R_{int} = 0.0403), of which 4330 are observed [$I > 2\sigma(I)$]. At final convergence R_1(obs.) = 0.0356, wR_2(all data) = 0.1044 for 407 parameters, GOF = 1.037. The residual electron density (min/max) is 0.313 / -0.292 eÅ^{-3}.

Crystal data for polymorph **C** at T = 130(2) K : $C_{26}H_{20}N_{14}S_2Fe$, M = 648.53, monoclinic, space group $P2_1/c$, a = 16.3109(4), b = 17.4820(5), c = 29.6431(5) Å, β = 90.847(1)º, V = 8452.0(3) Å^3, Z = 12, F(000) = 3984, D_{cacld} = 1.529 g cm^{-3}, μ(Mo–K$_\alpha$) = 0.730 mm^{-1}, 2θ_{max} = 54.94°. Red-brown in block (0.45 × 0.30 × 0.20 mm^3). 46384 total reflections, 18410 independent reflections (R_{int} = 0.0530), of which 11301 are observed [$I > 2\sigma(I)$]. At final convergence R_1(obs.) = 0.04462, wR_2(all data) = 0.1149 for 1201 parameters, GOF = 1.021. The residual electron density (min/max) is 0.349 / -0.396 eÅ^{-3}.

ADDSYM actually suggests that the cell is triple the size as it needs to be; however it is exactly due to the commensurate structure. The reason for the error message is due to the fact that extra molecules in the commensurate structure are only moved slightly away from their original positions in the non-commensurate structure. Nevertheless the extra reflections in the c* direction (h, k, l where l = 3n+1 and 3n+2) is quite apparent.

The reason for the low data completeness is due to the closeness of the nozzle of Helix system and the sample which limits part of the angular motion.

Crystal data for polymorph **C** at T = 60(2) K : $C_{26}H_{20}N_{14}S_2Fe$, M = 648.53, monoclinic, space group $P2_1/c$, a = 16.3266(2), b = 17.4800(4), c = 9.6827(4) Å, β = 91.112(1)º, V = 2762.82(13) Å^3, Z = 4, F(000) = 3984, D_{cacld} = 1.559 g cm^{-3}, μ(Mo–K$_\alpha$) = 0.744 mm^{-1}, 2θ_{max} = 55.50°. Red-brown in block (0.45 × 0.30 × 0.20 mm^3). 23421 total reflections, 6155 independent reflections (R_{int} = 0.0299), of which 5546 were observed [$I > 2\sigma(I)$]. At final convergence R_1(obs.) = 0.0263, wR_2(all data) = 0.0660 for 407 parameters, GOF = 1.036. The residual electron density (min/max) is 0.369 / -0.454 eÅ^{-3}.

The reason for the low data completeness is due to the closeness of the nozzle of Helix system and the sample which limits part of the angular motion.

Crystal data for thermally quenched state of polymorph **C** at T = 25(2) K : $C_{26}H_{20}N_{14}S_2Fe$, M = 648.53, monoclinic, space group $P2_1/c$, a = 16.2391(4), b = 17.3845(4), c = 29.6127(5) Å, β = 90.660(1)º, V = 8359.6(3) Å^3, Z = 12, F(000) = 3984, D_{cacld} = 1.546 g cm^{-3}, μ(Mo–K$_\alpha$) = 0.738 mm^{-1}, 2θ_{max} = 54.94°. Red-brown block (0.45 × 0.30 × 0.20 mm^3). 49898 total reflections, 18518 independent reflections (R_{int} = 0.0590), of which 12242 were observed [$I > 2\sigma(I)$]. At final

convergence R_1(obs.) = 0.0445, wR_2(all data) = 0.1030 for 1201 parameters, *GOF* = 1.024. The residual electron density (min/max) is 0.433 / -0.441 eÅ^{-3}.

The reason for the low data completeness is due to the closeness of the nozzle of Helix system and the sample which limits part of the angular motion.

Crystal data for polymorph **D** at T = 300(2) K: $C_{26}H_{20}N_{14}S_2Fe$, M = 648.53, monoclinic, space group $P2_1/c$, a = 10.8028(10), b = 15.9264(7), c = 17.4513(18) Å, β = 106.809(7)º, V = 2874.1(4) Å^3, Z = 4, F(000) = 1328, D_{cacld} = 1.499 g cm^{-3}, μ(Mo–K$_\alpha$) = 0.715 mm^{-1}, $2\theta_{max}$ = 55.00°. Red-brown needle (0.40 × 0.12 × 0.08 mm^3). 28211 total reflections, 6581 independent reflections (R_{int} = 0.0648), of which 3630 are observed [$I > 2\sigma(I)$]. At final convergence R_1(obs.) = 0.0474, wR_2(all data) = 0.1075 for 407 parameters, *GOF* = 1.008. The residual electron density (min/max) is 0.545 / -0.554 eÅ^{-3}.

Crystal data for polymorph **D** at T = 90(2) K: $C_{26}H_{20}N_{14}S_2Fe$, M = 648.53, monoclinic, space group $P2_1/c$, a = 10.8074(5), b = 15.7251(10), c = 17.0180(7) Å, β = 107.652(4)º, V = 2755.9(2) Å^3, Z = 4, F(000) = 1328, D_{cacld} = 1.563 g cm^{-3}, μ(Mo–K$_\alpha$) = 0.746 mm^{-1}, $2\theta_{max}$ = 55.00°. Dark-brown needle with size of 0.40 × 0.12 × 0.08 mm^3. 25192 total reflections, 6302 independent reflections (R_{int} = 0.0712), of which 4185 are observed [$I > 2\sigma(I)$]. At final convergence R_1(obs.) = 0.0434, wR_2(all data) = 0.0961 for 407 parameters, *GOF* = 1.002. The residual electron density (min/max) is 0.386 / -0.595 eÅ^{-3}.

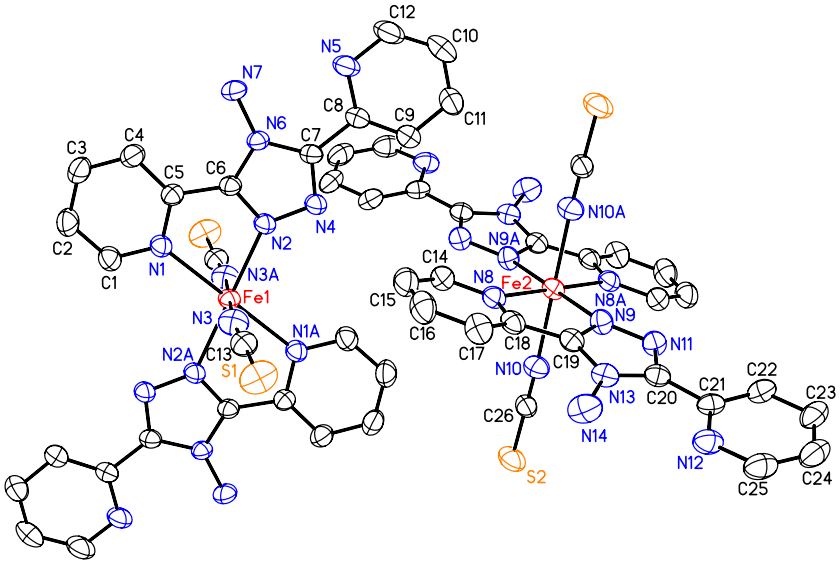

Figure S1. ORTEP diagram of *trans*-[Fe(abpt)$_2$(NCS)$_2$] polymorph **C** with atomic labelling and 30% probability in thermal ellipsoids at 300 K

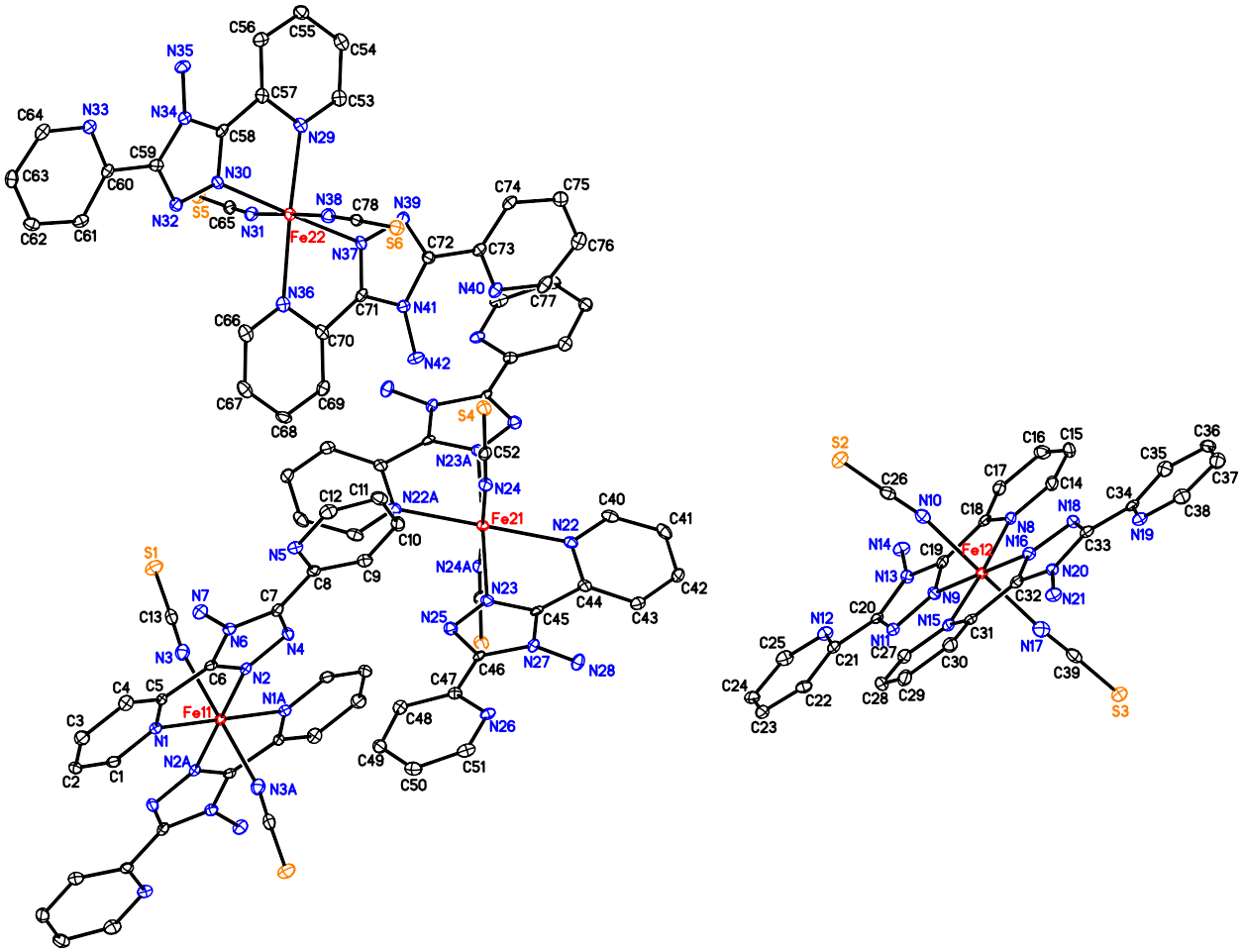

Figure S2. ORTEP diagram of *trans*-[Fe(abpt)$_2$(NCS)$_2$] polymorph **C** with atomic labelling and 50% probability in thermal ellipsoids at thermally quenched state at 25K

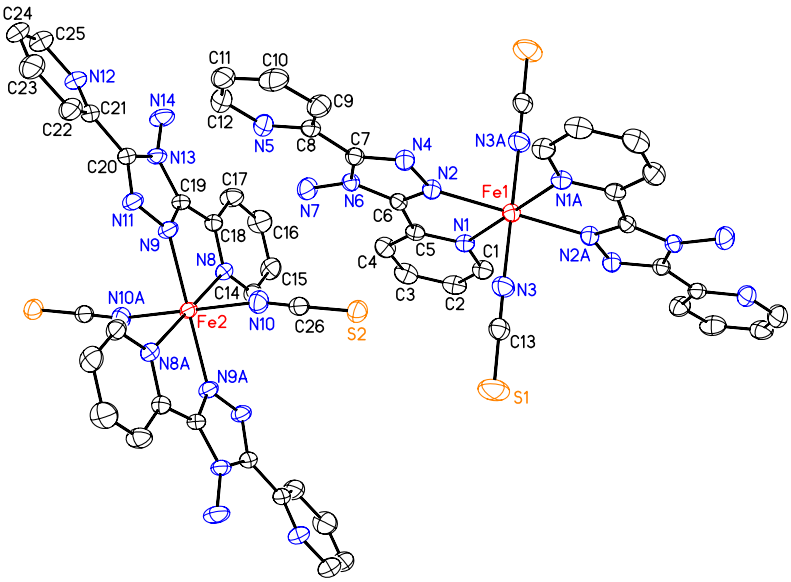

Figure S3. ORTEP diagram of *trans*-[Fe(abpt)$_2$(NCS)$_2$] polymorph **D** with atomic labelling probability in 30% thermal ellipsoids at 300 K

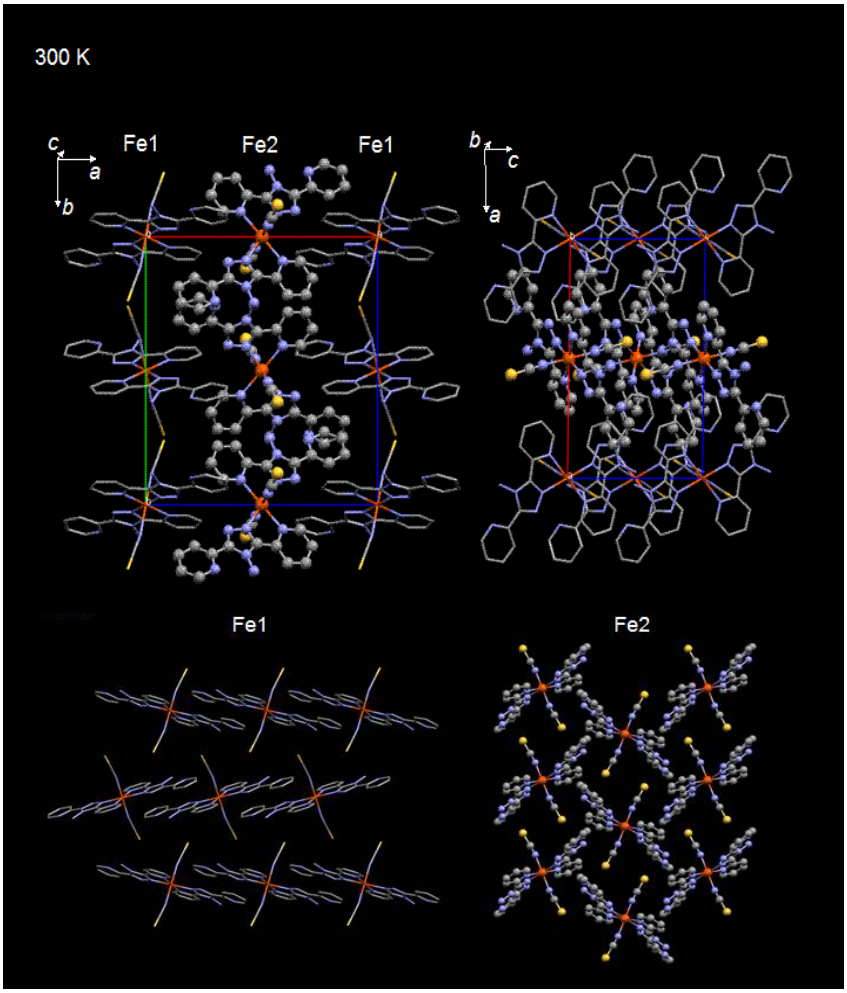

Figure S4. Packing diagram of polymorph **C**, site Fe1 are displayed in capped sticks form and site Fe2 are in ball and stick form.

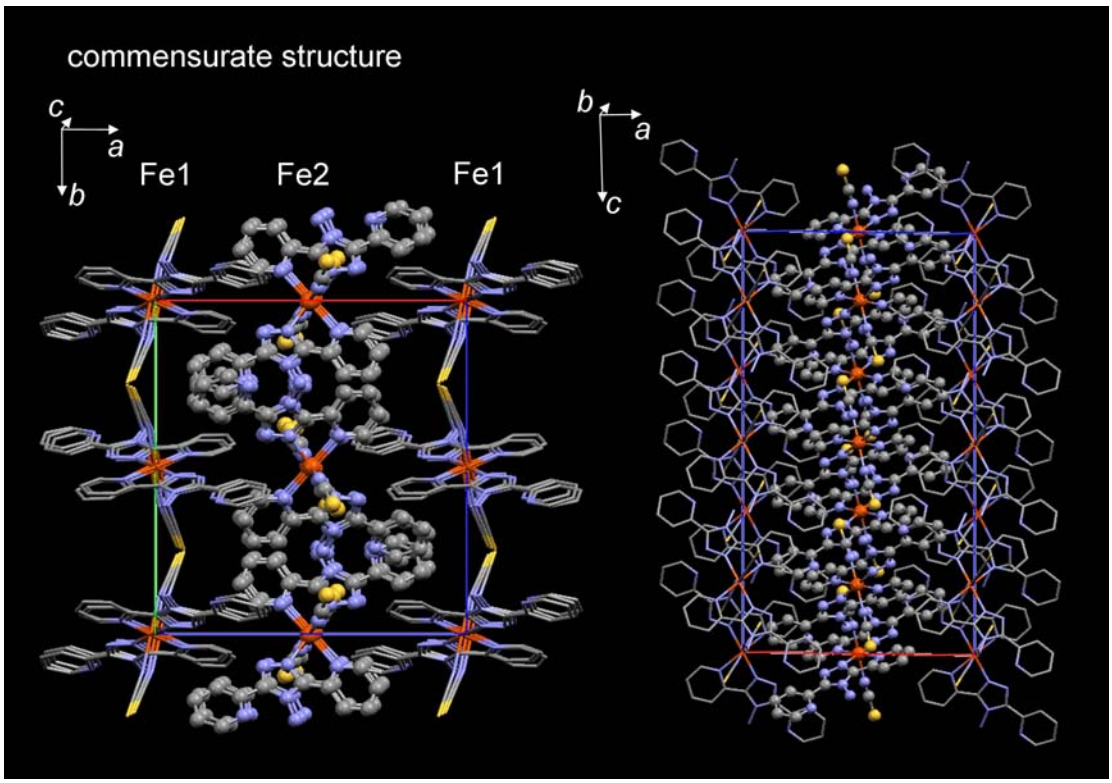

Figure S5. Packing diagram of polymorph **C** in the commensurate modulated phase, site Fe1 are displayed in capped sticks form and site Fe2 are in ball and stick form.

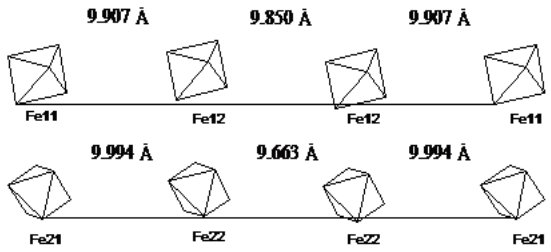

Fe11,Fe12 (top) and Fe21,Fe22 (bottom) view along b axis

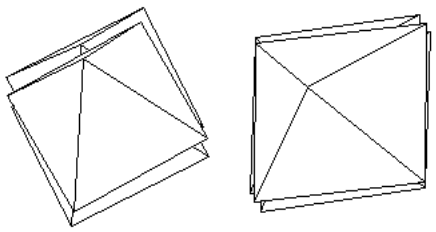

Movement of Fe (Å)				
		Along *a*	Along *b*	Along *c*
25 K	Fe12	0.34	0.05	0.03
HS3	Fe22	0.16	0.09	0.05
130 K	Fe12	0.25	0.05	0.03
	Fe22	0.12	0.08	0.11

Fe11,Fe12 (left) and Fe21,Fe22 (right) view along c axis

Figure S6. The displacements of molecules in the commensurate modulated phase from the original phase of polymorph **C** .

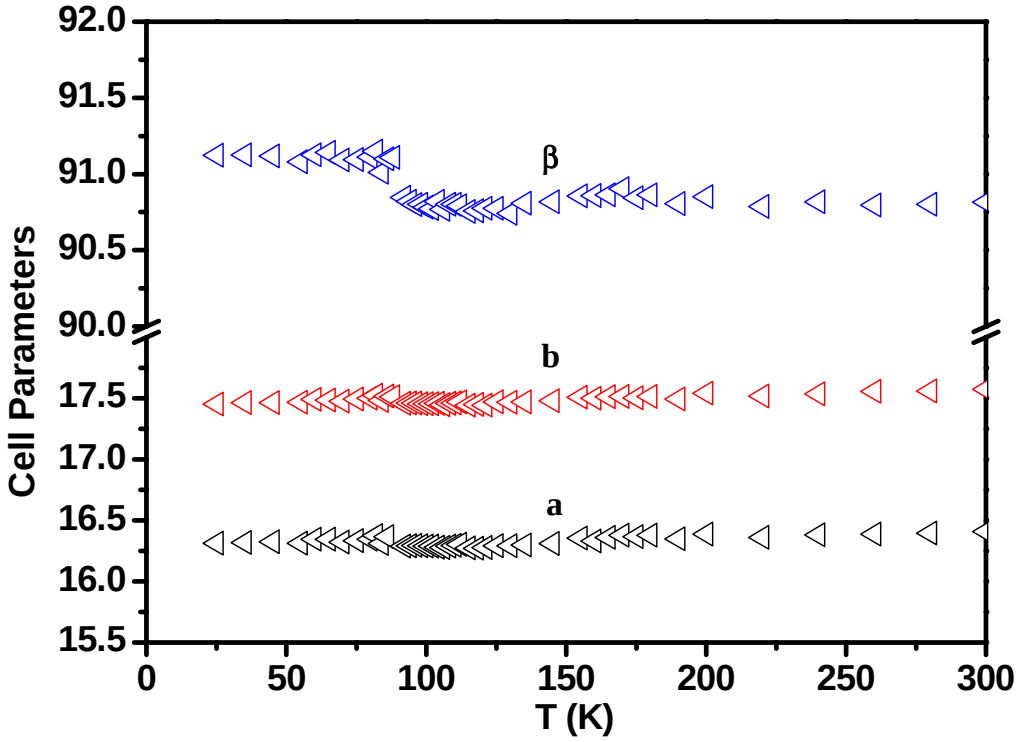

Figure S7 Temperature dependence of cell parameter *a*, *b* (Å) and *β* (deg) of polymorph **C**.

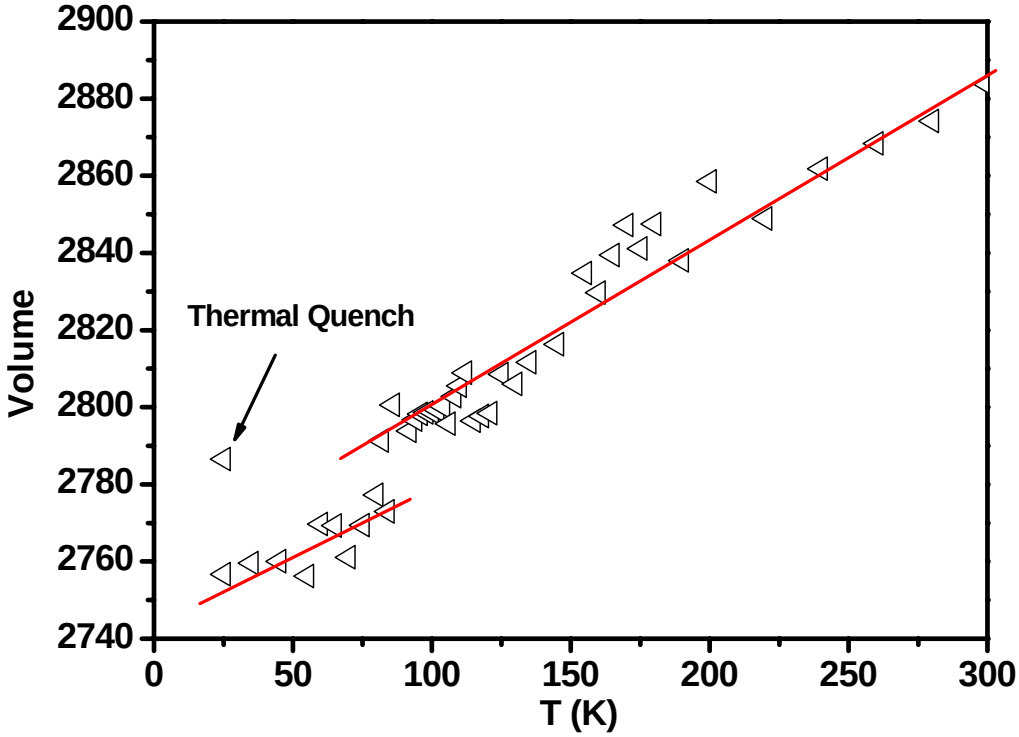

Figure S8 Temperature dependence of volume (Å^3) for polymorph **C.** For those at commensurate phase (thermally quenched 25K and 86-170 K), the volume is divided by 3 to bring into the same scale as the normal phase.

Table S1. Intra-ligand dihedral angles and the corresponding magnetic behavior. A = the coordinated pyridyl ring, B = the triazole ring and C = the uncoordinated pyridyl ring

Polymorph	T_C (K)	Dihedral angle A-B (deg)	Dihedral angle B-C (deg)	Magnetic behavior
A	188	7.9	8.3	Spin crossover
B	-	6.7	34.9	Paramagnetic
C				
site Fe1	86	5.6	0.1	Spin crossover
site Fe2		13.3	13.2	Paramagnetic
D				
site Fe1	162	2.5	6.2	Spin crossover
site Fe2		7.6	20.1	Paramagnetic

Table S2. The closest inter-ligand π-π distances between adjacent abpt ligands

Polymorph	T (K)	Closest inter-ligand π-π distances (Å)
A	293	3.366
B	293	3.528
C	300	3.532
Quenched	25	3.425
Relaxed	60	3.473
	130	3.457
D	300	3.482
	90	3.382